SEMI-ACTIVE CONTROL OF A METALLIC SCALED FRAME WITH A MR DAMPER: NUMERICAL AND EXPERIMENTAL RESEARCH

M.T. BRAZ-CÉSAR
I.P.B
Instº Politº Bragança
Bragança – Portugal

R. BARROS
F.E.U.P.
Fac.Eng. Univ. Porto
Porto – Portugal

ABSTRACT

The need of vibration control has been spreading in the last two decades to new application fields such as in the dynamic response of civil engineering structures. In this specific field a promising new technology for control of structural vibrations is based on the use of magneto-rheological (MR) fluid devices in the so-called MR dampers. The present work describes part of the R&D on using a semi-active structural control technique in a civil engineering experimental model frame equipped with a MR damper, developed within COVICOCEPAD project approved in the framework of Eurocores program S3T. Some results are provided associated with the calibration of a MR damper at FEUP as well as on the experimental modal identification of the dynamic properties of a small-scale metallic frame, without and with inclusion of a specific MR device. Some numerical results of the controlled frame under simulated earthquakes are given, to be later compared with the experimental results of such frame installed in a Quanser shaking table.

Keywords: Control of Vibrations for Smart Structures, Semi-Active Devices, MR Dampers, Experimental Tests on Shaking Table.

1. INTRODUCTION

Structural control has an extensive and successfully history in mechanical, aerospace and related engineering fields. The vast quantity of successful applications in these knowledge areas lead to the opening of new research paths namely in civil engineering structures. However the application of structural control techniques to the response of large civil

engineering structures is more challenging due to the amount of energy involved in the control process arising from environmental actions such as strong wind or seismic excitation.

In the last two decades R&D of structural vibration control devices for buildings and bridges has been intensified to reply to construction market needs that demand more effective systems to decarease the damage caused by seismic and wind loading. This orientation is the result of a public necessity to guarantee the serviceability of construction lifelines throughout and after the occurrence of a moderate or severe seismic event (Barros et al. [1] [2]). Although the main purpose of a seismic design is to protect the population from the consequences of a severe earthquake, the protection of investment may also be regarded as an important option during the conception and design process.

Seismic isolation and passive energy dissipation are two well-established techniques validated by a huge amount of real applications. The potential of structural control to reduce the response of large buildings to strong wind excitation has been largely realized using passive tuned mass dampers (TMD's) or active mass dampers.

However, passive systems are tuned to have specific dynamic property and therefore some uncertainties about the response under large earthquakes remains. To avoid this matter, active control systems for structural vibration mitigation for wind and traffic excitations were developed and have been successfully implemented in real applications. Basically the control system for civil engineering applications must be able to respond fast enough to a control signal in order to generate high dissipative forces with low power supply.

In this context, magneto-rheological fluid based devices have the appropriate features to satisfy all these requirements justifying the relevance of these for possible civil engineering applications and therefore the attention of researchers to study its potential as vibration control hardware. In addition, the control strategy for these devices is based on semi-active control that may be more reliable and stable than active control.

In this paper is addressed some on-going R&D on the vibration control of a 3-DOF scaled metallic frame with a MR damper. An equivalent device was tested in the laboratory to obtain the main rheological characteristics in order to develop a numerical model to simulate its behaviour. Then a 3-DOF scaled frame was assembled and system identification techniques using an impact hammer procedure were performed to obtain the experimental dynamic properties of this structural system. The MR damper was then assembled in the scaled frame and a new identification procedure was carried out to verify the influence of this device (without and with internal coil electrical current) in the frame dynamic behaviour. Based on these results a numerical model was created to initiate the semi-active control research process in order to investigate and calibrate the frame behaviour with the MR damper.

2. PASSIVE AND SEMI-ACTIVE CONTROL OF STRUCTURES

2.1 Passive control using base isolation (BI)

The strategies based upon passive control – namely the base isolation (BI) systems, shock absorbers (SA) and tuned mass dampers (TMD) – are well known and accepted methodologies due to its effectiveness as a mitigation approach for dynamic loading.

The easiest and cheapest way to protect a structure from undesired vibration is to add a passive isolation system to reduce the response in some sensitive region. Figure 1 shows a single degree-of-freedom isolator, modelled by the transmissibility transfer function:

$$T = \frac{x_p}{x_b} = \frac{\dot{x}_p}{\dot{x}_b} = \frac{\ddot{x}_p}{\ddot{x}_b} = \frac{1 + 2\xi_p \dfrac{s}{\omega_n}}{1 + 2\xi_p \dfrac{s}{\omega_n} + \dfrac{s^2}{\omega_n^2}} \tag{1}$$

where s is the Laplace variable, ω_n is the natural frequency, ξ is the passive damping ratio, x_p and x_b are the payload and base displacements. The transmissibility modulus and phase for several damping ratios are also shown in Figure 1 (Barros et al. [3]). In this figure it is visible that at low passive damping ratios, the resonant transmissibility is relatively large while at frequencies above resonant peak it is quite low; and the reverse is also true for relatively high damping ratios.

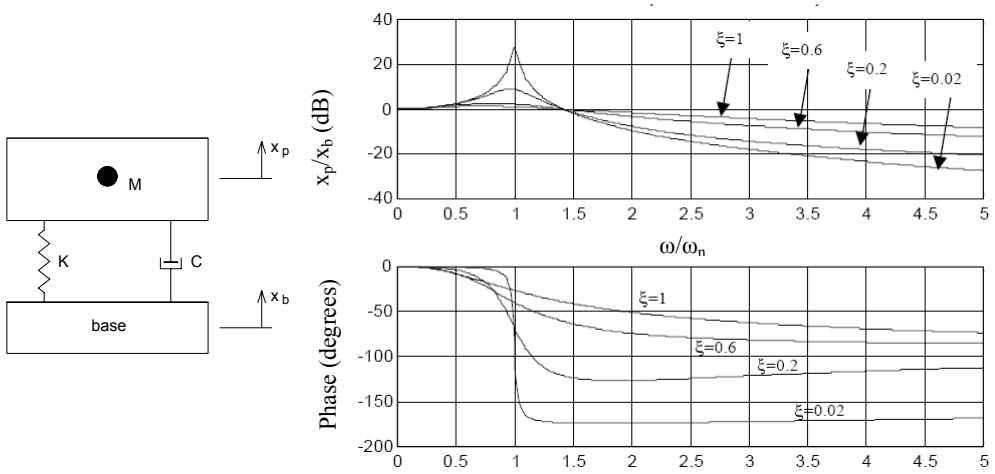

Figure 1: Passive 1-DOF isolator and transmissibility transfer function.

The base isolation system is the first approach in the analysis of structures with passive energy dissipation devices and is based on the use of a model with 2 (translational) DOF represented in Figure 2. The background to this work was based on Naeim and Kelly [4] and Soong and Dargush [5] that resumes the theory of seismic isolation and the design of seismic isolated structures, within the framework of existing codes. In this context such model was used earlier

by Barros and Cesar [6] , Cesar and Barros [7]. Also Figueiredo and Barros [8] have addressed the importance of the influence of increasing damping in seismic isolation.

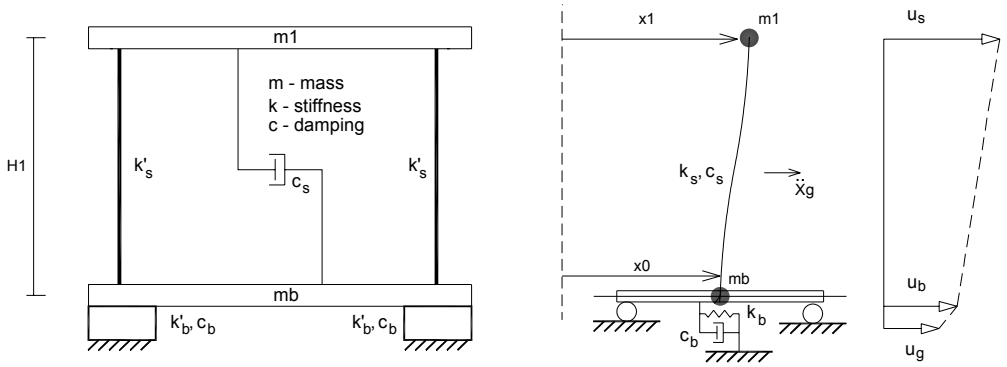

Figure 2: Passive energy dissipation at the base of the structure (Base Isolation).

The classical design approach for the base isolation devices accounting horizontal seismic component is also shown in Figure 2. In this case the equation of motion (2) has the matrix identifications (mass, damping and stiffness matrices) given in equation (3), where c_b is the damping coefficient of the isolation system, c_s is the damping coefficient of the fixed structure and k_s is the stiffness of the fixed-base structure.

$$M\ddot{X}(t) + C\dot{X}(t) + KX(t) = -M\{I\}a(t) \tag{2}$$

$$M = \begin{bmatrix} m_b & 0 \\ 0 & m_1 \end{bmatrix},\ C = \begin{bmatrix} c_b + c_s & -c_s \\ -c_s & c_s \end{bmatrix},\ K = \begin{bmatrix} k_b + k_s & -k_s \\ -k_s & k_s \end{bmatrix} \tag{3}$$

Base isolation devices are made of natural rubber that guarantees damping ratios in the order of 10-20% of critical damping, considerably bigger than structural damping ratios for steel frames (in the order of 2%). In our study a vibration absorbing mounting similar to those used for machine isolation is used to simulate the base isolation system. Because this simplified passive system has an insignificant energy dissipation – an important characteristic for real building applications – the expected structural behaviour remains the same as for a real base system; so the main purpose of a base isolation system is to increase the structural flexibility and consequently the main period to a more secure range, in which resonance effects are significantly lower (and often irrelevant) becoming a type of pseudo-filter [2] [4] [5] [6]. Studies on the optimal design of base-isolators for multi-storey buildings were also successfully developed (Baratta and Corbi [9] [10]), as was also synthesized collectively (Barros et al. [3]).

However, the limitations that these devices/methodologies have to allow variations of the dynamic loading or structural parameters encouraged the study and development of more advanced control systems based on active, semi-active or hybrid control devices (Figure 3).

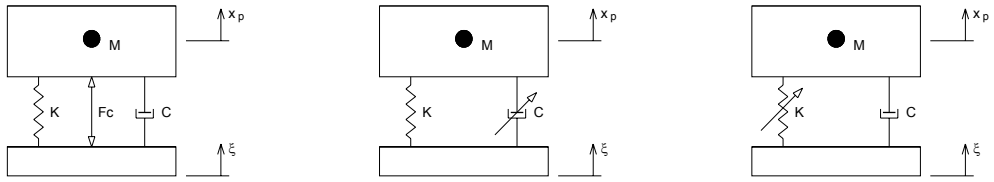

Figure 3: Active and semi-active vibration control strategies.

The numerical models used to simulate this new type of control in civil engineering structures allow to conclude that it is possible to apply them successfully but some experimental research is required to validate these models in order to be accepted as a possible structural vibration control solution. Also, the practical application of active control to some civil engineering structures can easily become analytically cumbersome for immediate implementation, as was emphasized by Barros [11] for the case of pipeline shell structures with ring stiffeners (but also of interest to fuselage structures as well).

Since active devices are not a practical and reliable option in the near future as a structural building or bridge control systems due to energy demand and possible failure in case of power loss, semi-active control devices gained significant attention by the civil engineering community in the last years because they have at the same time the benefits of passive and active devices without requiring a huge amount of energy to work properly.

2.2 Semi-active control with MR dampers

The next stage is to use semi-active devices to control the vibration of a base excited structure. Among the possible semi-active technologies, the magneto-rheological fluid based devices are seen as a promising solution for structural control (Barros et al. [3], Barros [12]).

Basically two types of rheological fluids can be used to create a structural control system: magneto-rheological (MR) and electro-rheological (ER) fluids. MR fluids are materials that exhibit a change in rheological properties with the application of a magnetic field while ER fluids exhibit rheological changes when an electric field is applied to the fluid.

Although power requirements are approximately the same MR fluids only require small voltages and currents while ER fluids require very large voltages and very small currents. However, ER fluids have many disadvantages including relatively small rheological changes and significant property changes with temperature. Thus, MR fluids have become an extensively studied “smart” fluid and some experimental research has been done in the last years to produce a “smart” control device with this fluid.

Usually, the MR fluid devices are built to operate in the following modes (Figure 4): valve mode or flow mode; direct shear mode or clutch mode; squeeze film compression mode and the combination of some of the previous modes.

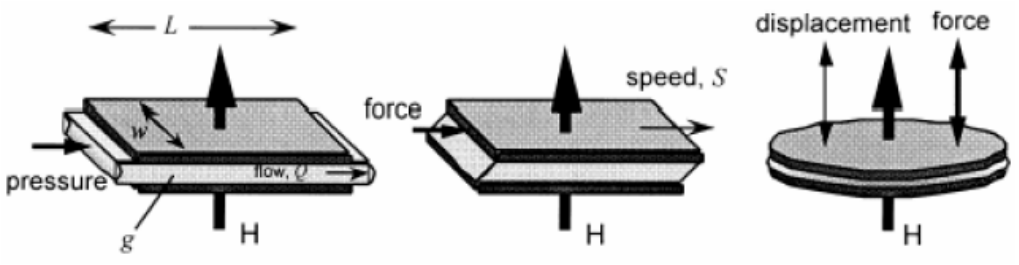

Figure 4: Basic operation modes of MR-fluid.

For vibration control purposes the "smart" MR fluid effect is interesting since it is possible to apply this phenomenon to create a variable damping device or a "smart" hydraulic damper. The current applied to a MR fluid essentially allows controlling the damping force without the need of mechanical valves that are commonly used in adjustable dampers. This offers the possibility to create a reliable damper since a failure in the control system reverts the MR damper to a passive damper (Figure 5).

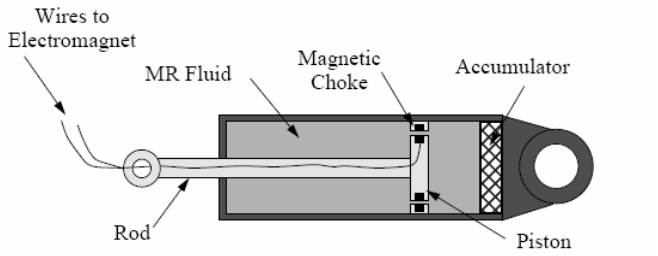

Figure 5: Schematic representation of a magneto-rheological damper.

The MR damper performance is often characterized by using the force vs. velocity relationship. Regular viscous damper has an ideal linear constitutive behaviour and the slope of the line is known as the damper coefficient. In the case of MR dampers the possibility to change the damping characteristics leads to a force vs. velocity envelope that can be described as an area rather than a line in the force-velocity plane. This behaviour is the fundamental condition to build a "smart" damper since it is possible to design a controller to follow any force-velocity relationship within the envelope to create a control strategy.

According to the available bibliography two common methods can be used to model MR devices such as MR dampers: the parametric modelling technique that characterizes the device as a collection of springs, dampers, and other physical elements; the non-parametric modelling that employ analytical expressions to describe the characteristics of the modelled devices. Many authors have developed modelling techniques for the MR dampers based on both methods. In recent studies Dyke et al [13] presented a simple parametric model based on the extension of the Bouc-Wen model that allows a good approximation to the real MR damper behaviour as shown in Figure 6.

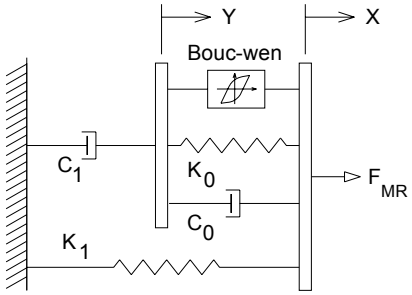

Figure 6: Modified Bouc-Wen model for a MR damper.

The Bouc-Wen model is based on the Markov-vector formulation to model nonlinear hysteretic systems and according with the modified model shown in Figure 6, the MR force can be computed by

$$F_{MR} = c_1\dot{y} + k_1\left(x - x_0\right) \tag{4}$$

$$\begin{cases} \dot{y} = \dfrac{1}{\left(c_0 + c_1\right)}\left\{\alpha z + c_0\dot{x} + k_0\left(x - y\right)\right\} \\ \dot{z} = -\gamma\left|\dot{x} - \dot{y}\right|z\left|z\right|^{n-1} - \beta\left(\dot{x} - \dot{y}\right)\left|z\right|^{n} + A\left(\dot{x} - \dot{y}\right) \end{cases} \tag{5}$$

In these equations z is the revolutionary variable, F_{MR} is the predicted damping force, k_1 is the accumulator stiffness, c_0 is the viscous damping observed at larger velocities and the parameters β, γ and A allows controlling the linearity in the unloading and the smoothness of the transition from the pre-yield to the post-yield region. The dashpot c_1 is included to produce the roll-off at low velocities, k_0 is used to control the stiffness at larger velocities, and x_0 is the initial displacement of spring k_1 associated with the nominal damper due to the accumulator.

$$\begin{cases} c_1 = c_{1a} + c_{1b}u \\ c_0 = c_{0a} + c_{0b}u \\ \alpha = \alpha_a + \alpha_b u \\ u = -\eta\left(u - v\right) \end{cases} \tag{6}$$

The damping constants c_0 and c_1 depend on the electrical current applied to the MR damper. The variable u is the current applied to the damper through a voltage-to-current converter with a time constant η and the variable v is the voltage applied to the converter. A simple MATLAB/SIMULINK block diagram can be used to simulate the Bouc-Wen model of a MR damper (Barros et al. [3]).

3. EXPERIMENTAL SETUP

3.1 MR damper

To study the behaviour of a MR damper some experiments were carried out on a MTS universal testing machine (Mechanical Engineering Laboratory at FEUP) with the MR damper device RD-1005-3 supplied by LORD Corporation (Figure 7).

According to the device specifications it has a capacity to provide a peak to peak force of 2224 N at a velocity of 51 mm/s with a continuous current supply of 1 A. The MR damper was tested using the computer-controlled servo hydraulic MTS universal testing machine shown in Figure 8. The MR damper was attached to the MTS machine (operating under displacement control mode) and a 5 kN load cell was incorporated at the upper head to measure the force applied to the damper. The results were automatically collected by the computer-controlled MTS equipment and stored in a desktop PC.

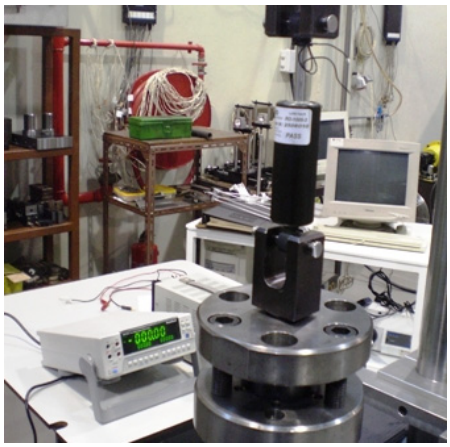

Parameter	Value
Extended length	208mm
Device stroke	±25mm
Max. Tensile force	4448N
Max. temperature	71ºC
Compressed length	155mm
Response time	<10ms
Max. Current supply	2A

Figure 7: Magneto-rheological damper RD-1005-03 test setup at FEUP.

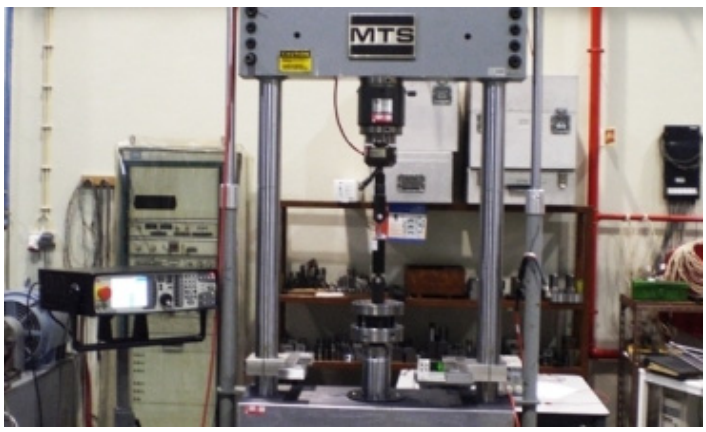

Figure 8: Magneto-rheological damper and MTS universal setup (FEUP).

After assemblage, the MR damper was forced with a sinusoidal signal at a fixed frequency, amplitude and current supply. To obtain the response of the MR damper under several combinations of frequencies, amplitudes and current supplies a series of tests were carried out. Therefore, a set of frequencies (0.5, 1.0, 1.5 and 2.0 Hz), amplitudes (2, 4, 6, 8 and 10 mm) and current supplies (0.0, 0.1, 0.2, 0.25, 0.5, 0.75, 1.0 and 1.5 A) were used to complete the test program (Barros et al. [3]).

In order to control and avoid temperature failure, especially at higher frequencies, a thermocouple was used to measure the external temperature of the MR damper. Typical results of this set-up of the experimental research are shown in Figures 9 and 10.

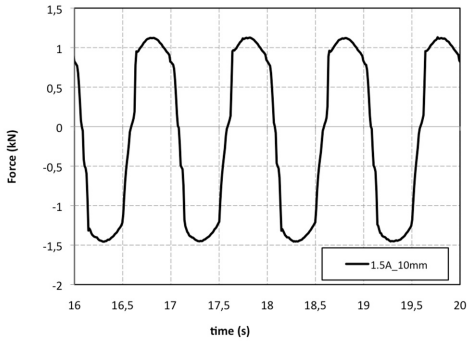

Figure 9: MR damper RD-1005-03 Force-Time History (1.5 A and 10mm).

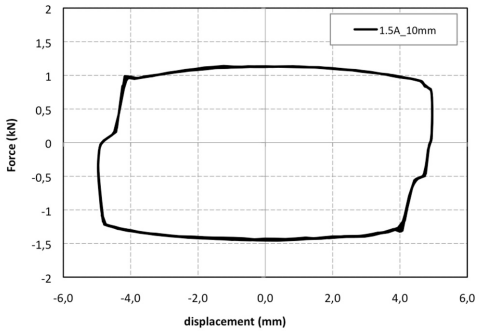

Figure 10: MR damper RD-1005-03 Force-Displacement curves (1.5 A and 10mm).

The variable current tests demonstrate that increasing the input current implies an increase in the force required to yield the MR fluid and a plastic-like behaviour in observed in the hysteretic loop. In the frequency dependent test is observed that the maximum damping force increases with the frequency due to large plastic viscous force at higher velocity.

3.2 Scaled metallic frame

According with the scheduled research program the next stage was related with study the experimental dynamic behaviour of a 3DOF scaled metallic load frame with and semi-active devices. Among the several possible control strategies that can be easily used with this scaled frame, Tuned Mass Dampers (TMD), Tuned Liquid Dampers (TLD) and a Base Isolation system (BI) are the more simple to implement due to its passive behaviour. However, the structural setup was developed to allow semi-active control that was performed with a MR damper connected horizontally at the first floor level. A hybrid control system, based on the association of base isolation and MR dampers, can be also considered in the research program but it will not be addressed in this study.

The experimental scaled building is a single bay three-storey frame (three degree of freedom in shear frame configuration) with the columns at the corner having the same stiffness as shown in Figure 11. The columns are made of aluminium with an average cross section of 1.5mm by

50mm and the diaphragm floors are made of polycarbonate plates monolithically attached to the columns. The frame mass is around 19 kg and each floor has an average mass of 3.65 kg. The stiffness of the experimental frame was designed to keep the fundamental frequency near to 2 Hz.

Assuming a three storey shear frame, the frame mass (M) and the stiffness matrix (K) are obtained as the following

$$M = \begin{bmatrix} 3.65 & 0 & 0 \\ 0 & 3.65 & 0 \\ 0 & 0 & 3.65 \end{bmatrix} (kg) \qquad K = \begin{bmatrix} 5820 & -2910 & 0 \\ -2910 & 5820 & -2910 \\ 0 & -2910 & 2910 \end{bmatrix} (N/m) \tag{7}$$

The three natural frequencies obtained with the above mass and stiffness matrices are: 2.00Hz, 5.60Hz and 8.09Hz. A damping of 0.5% along with the above mass and stiffness matrices formed the initial parameters for the modal analysis.

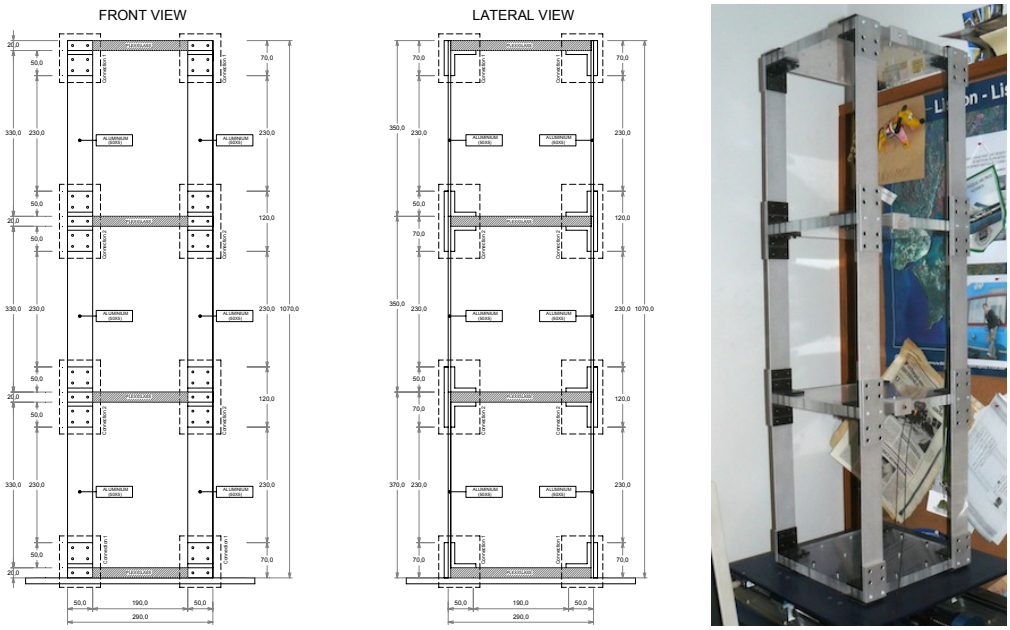

a) geometrical properties b) perspective view

Figure 11: Metallic scaled frame (FEUP).

This experimental frame located at FEUP-Covicocepad Lab, can be forced dynamically using the Quanser shaking table II shown in Figure 12 as the dynamic loading actuator.

The experimental research can employ three control strategies: (1) a passive control based on base isolation devices; (2) a semi-active control based on a MR damper assembled to the structure; (3) a hybrid control technique through the association of the base isolation devices with the MR damper (Barros et al. [3]).

Figure 12: Quanser shaking table II (and its controllers) at FEUP – Covicocepad Lab.

To study the semi-active control strategy a small MR damper was placed horizontally at the first floor level attached to the frame and rigidly attached to the shaking table as shown in Figure 13. To acquire the damping force generated during the experimental tests a load cell is placed in the MR damper support system.

Figure 13: MR damper attached to the experimental metallic frame.

The small size and mass of the scaled frame does not allow the use of RD-1005 MR damper since the force range of this device is beyond the dynamic forces expected during the experimental research. Therefore, a small MR damper shown in Figure 14 was used (RD-1097 from Lord Corp.) gently provided by Prof. Vincenzo Gattulli from D.I.S.A.T, L'Aquilla University in Italy.

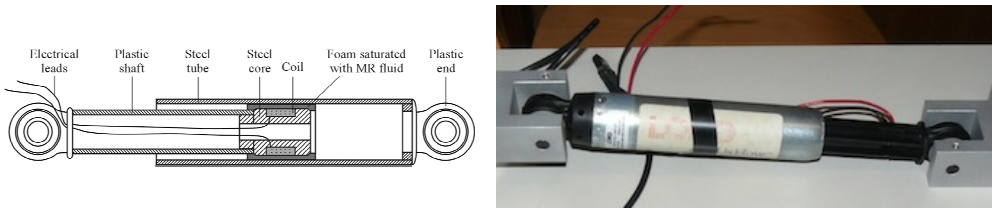

Figure 14: RD-1097 MR damper from Lord Corp.

The main parameters of this device listed by the manufacturer are: minimum force in passive-off mode < 9 N (for current 0.0A at piston velocity 200 mm/s), maximum force 100 N (for current 1.0A and piston velocity 51 mm/s), stroke ±25 and response time < 25 ms (time required to reach 90% of the steady-state value of force under a step change of the current from 0.0 to 1.0A, for 51 mm/s).

4. SYSTEM IDENTIFICATION

4.1 Scaled metallic frame

In this section the details of the parameter identification of the metallic frame alone (without the MR damper/metallic frame association) are presented.

An impulse hammer test was carried out in order to obtain the dynamic behaviour of the structure in response to an applied excitation. The main purpose was to obtain the transfer function or Frequency Response Function (FRF) of the experimental frame (Figure 15). The structural response was measured with a piezoelectric accelerometer (Bruel & Kjaer type 4393 with measuring amplifier type 2525) placed at the first floor and a portable real-time Analyzer (OROS 35 real-time multi-analyzer) that was used to perform the necessary mathematical rationing on input and response signals to produce the desired transfer function. To perform the identification an impulsive force was given with the impact hammer at the centre of each floor plate and the acceleration response was measured at the first floor plate along the direction of the impulse.

Figure 15: Identification and acquisition hardware.

The desired frequency response functions (magnitude and phase) for each input/output measurement are shown in Figures 16-18.

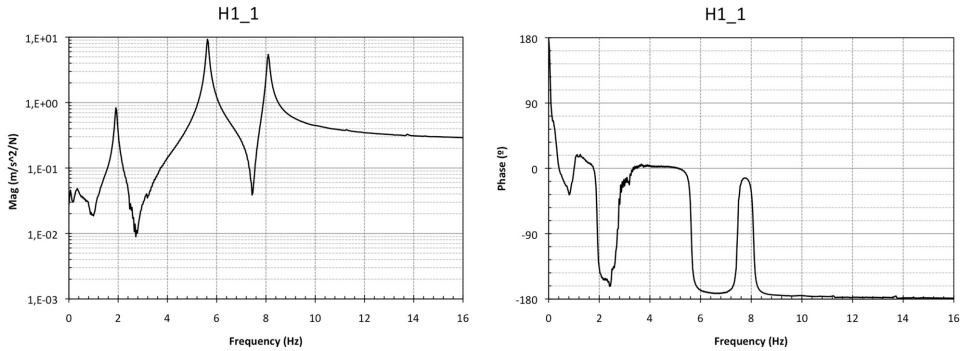

Figure 16: FRF magnitude and phase of H1_1.

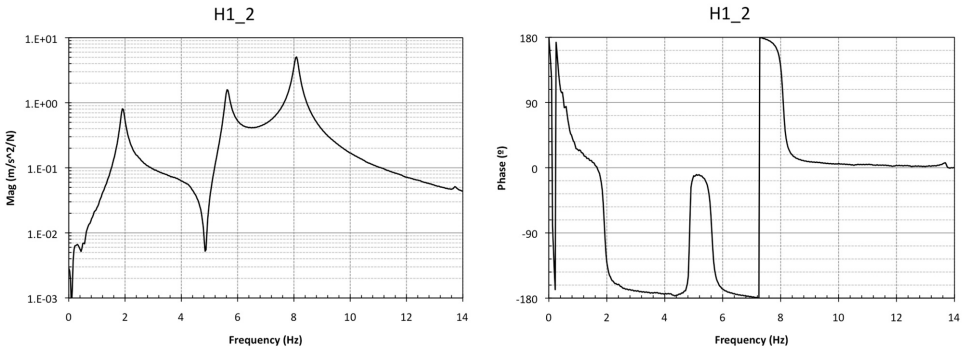

Figure 17: FRF magnitude and phase of H1_2.

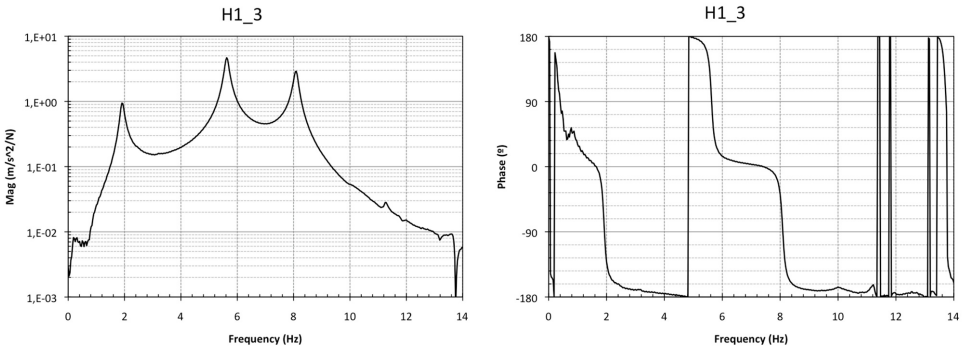

Figure 18: FRF magnitude and phase of H1_3.

The parameters of the scaled frame were then obtained based on the data provided by these functions and are tabulated in Table 1.

Table 1: Parameters of the scaled frames

	Frequency	Damping	Modal Participation
Mode 1	1,913986	0,03157	34,43248
Mode 2	5,627778	0,01198	35,25975
Mode 3	8,086245	0,00899	30,30777

Once the modal parameters are determined, several procedures can be used to validate modal data. In this case, the Modal Assurance Criterion (MAC) was used in order to compare analytical and experimental results. The function of the MAC is to provide a measure of consistency (degree of linearity) between estimates of a modal vector. This function is defined by the following expression (Ewins [14]):

$$MAC_{j,k} = \frac{\left(\left[\phi_j^m\right]^T \left[\phi_k^a\right]\right)^2}{\left(\left[\phi_j^m\right]^T \left[\phi_j^m\right]\right)\left(\left[\phi_k^a\right]^T \left[\phi_k^a\right]\right)} \tag{8}$$

This provides an additional confidence factor in the evaluation of a modal vector from different excitation locations or different modal parameter estimation algorithms. Applying this procedure the following MAC matrix was obtained

$$MAC = \begin{bmatrix} 1.000 & 0.501 & 0.031 \\ 0.501 & 1.000 & 0.228 \\ 0.031 & 0.228 & 1.000 \end{bmatrix} \tag{9}$$

The MAC takes on values from zero, representing no consistent correspondence, to one, representing a consistent correspondence. Therefore, if the modal vectors under consideration truly exhibit a consistent relationship, the modal assurance criterion should approach unity and the value of the modal scale factor can be considered to be reasonable.

4.2 Scaled metallic frame with the MR damper

To study the influence of the MR damper in the dynamic behaviour of the structural system, a new identification procedure was carried out after connecting the MR damper to the experimental frame as shown in Figure 19. A load cell was also attached to the system allow measuring the generated axial force in the MR damper.

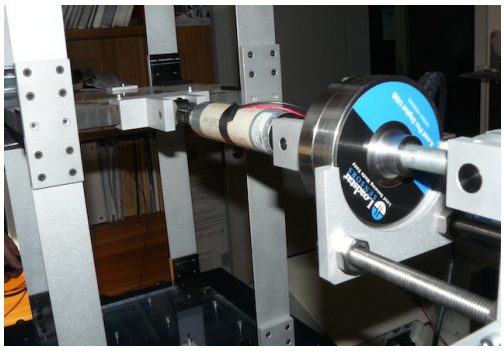

Figure 19: MR damper and load cell.

The identification was carried out with three different current intensities (or damping): passive-off or 0.0A, passive with 0.5A and passive with 1.0A. The FRF for each input/output measurement for the passive-off configuration are shown in Figures 20-22.

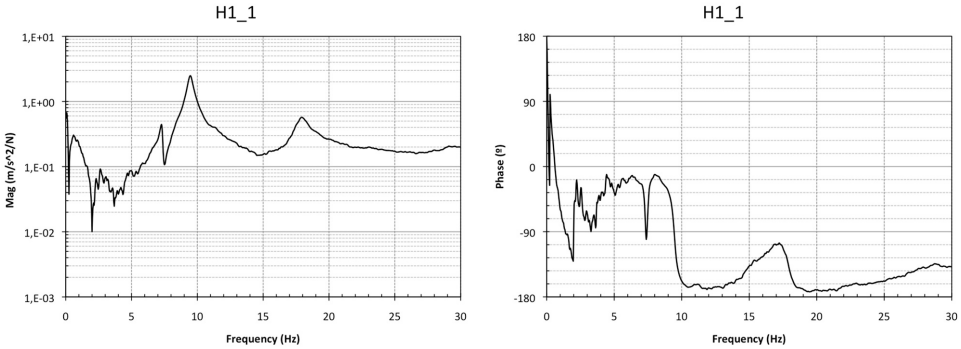

Figure 20: FRF magnitude and phase of H1_1 with MR damper at 0.0A.

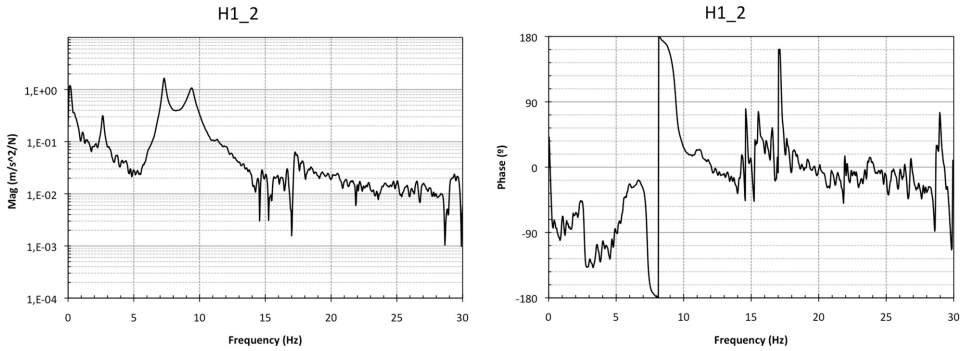

Figure 21: FRF magnitude and phase of H1_2 with MR damper at 0.0A

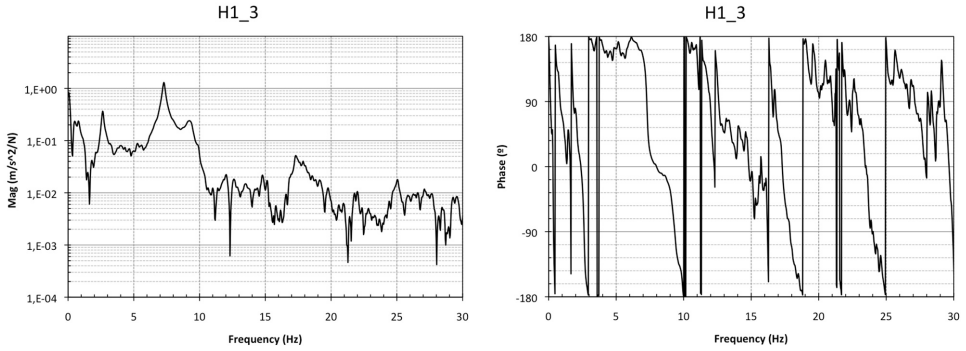

Figure 22: FRF magnitude and phase of H1_3 with MR damper at 0.0A

A simple study of the FRF functions allows concluding that the inclusion of the MR damper changes the natural frequencies and more obviously the amount of structural damping. The frequencies were slightly shifted to higher values since the MR damper adds stiffness to the system and the expected damping properties of a device as a damper significantly reduce the time response. Furthermore, after placing the MR damper in the frame the system begins to perform as a 2-DOF since the first floor displacement (were the MR damper was placed) decreases significantly.

The identification procedure was then performed for the other passive configurations (for 0.5 A and 1.0 A). Since the results revealed basically the same structural performance for the two configurations, only the results for the passive system with 0.5A are shown in Figures 23-25. The same conclusions as for the passive-off system can be applied to the new MR damping performance. It was clear that the increase of current of the MR damper, changes the frame stiffness and lead to even more substantial 2-DOF system behaviour.

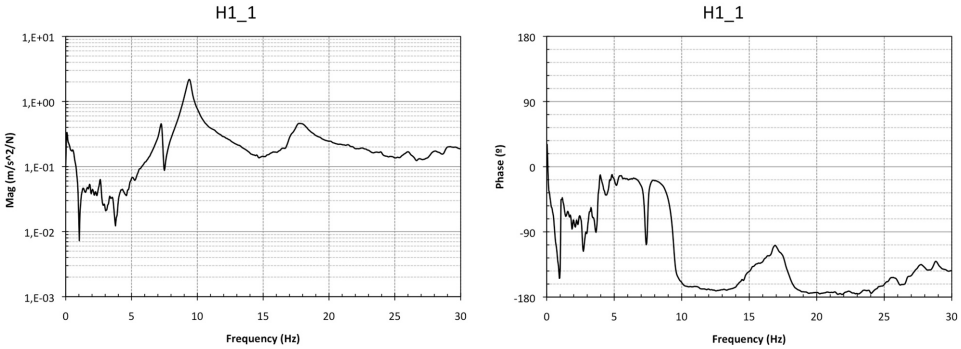

Figure 23: FRF magnitude and phase of H1_1 with MR damper at 0.5A.

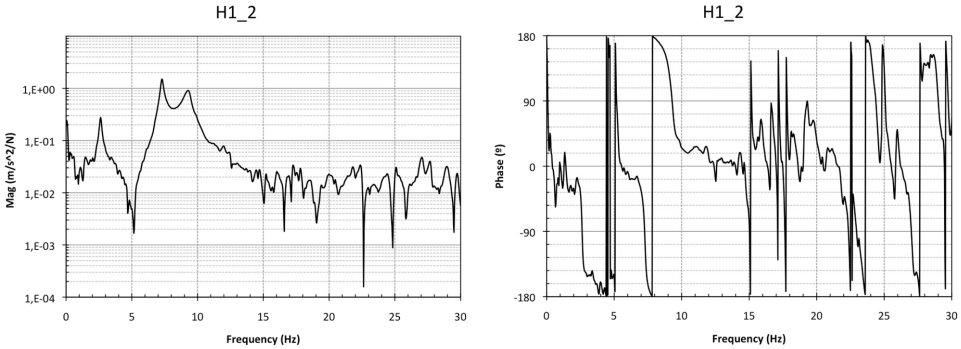

Figure 24: FRF magnitude and phase of H1_2 with MR damper at 0.5A.

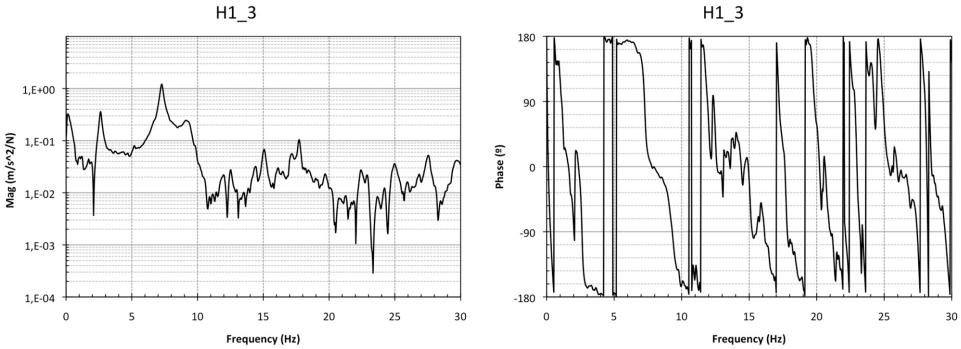

Figure 25: FRF magnitude and phase of H1_3 with MR damper at 0.5A.

5. SEMI-ACTIVE CONTROL

The equation of motion that describes the behaviour of a controlled building under an earthquake load (Barros et al. [3]) is given by:

$$M\ddot{x} + C\dot{x} + Kx = -\Gamma f - M\lambda\ddot{x}_g \tag{10}$$

where M is the mass matrix, C is the damping matrix, K is the stiffness matrix, x is the vector of floors displacements, $\dot{x}$ and $\ddot{x}$ are the floor velocity and the acceleration vectors respectively, f is the measured control force, λ is a vector of ones and Γ is a vector that accounts for the position of the MR damper in the structure.

This equation can be rewritten in the state-space form as

$$\dot{z} = Az + Bf + E\ddot{x}_g \tag{11}$$

$$y = Cz + Df + v \tag{12}$$

where z is the state vector, y is the vector of measured outputs and v is the measurement noise vector. The other matrix quantities are defined by

$$\begin{aligned} A &= \begin{bmatrix} 0 & I \\ -M^{-1}K & -M^{-1}C \end{bmatrix} \qquad B = \begin{bmatrix} 0 \\ M^{-1}\Gamma \end{bmatrix} \quad E = -\begin{bmatrix} 0 \\ \lambda \end{bmatrix} \\ C &= \begin{bmatrix} -M^{-1}K & -M^{-1}C \\ I & 0 \end{bmatrix} \qquad D = \begin{bmatrix} M^{-1}\Gamma \\ 0 \end{bmatrix} \end{aligned} \tag{13}$$

To control this semi-active structure based on a control force determination, usually are measured: the absolute acceleration of some relevant selected points in the structure; the displacement of the control device; and the control force.

5.1 Control algorithms

After calibrating the MR damper numerical model it is necessary to select a proper control algorithm to efficiently use this device in reducing the dynamic response of structural systems. Obviously, the control strategy depends on the MR damper model selected to simulate the nonlinear hysteretic behaviour of this device (Jansen and Dyke [15], Kang-Min et al. [16]).

The fundamental condition to operate the MR damper is based on a generated damping force that is related with the input voltage; the control strategy is selected so that the damping force can track a desired command damping force. The available models can be categorized in static and dynamic models. The basic difference between them is that the static models do not include dynamic relation between input and output.

As mentioned before this work is based on the Bouc-Wen model (Dyke et al. [13]) that can represent the hysteresis dynamics explicitly. Therefore, an efficient control algorithm must be

developed or chosen from the available research bibliography to correctly characterize the intrinsic MR fluid behaviour, maximizing the MR damper characteristics as a semi-active control device (Barros et al. [3]).

In the last few years several approaches have been proposed and intensively studied for better selection of the input voltage that must be applied to the MR damper to achieve the maximum performance. Among the proposed strategies the following are the most studied: Lyapunov Based Control; Decentralized Bang-Bang Control; LQG (Linear Quadratic Gaus-sian) or Clipped-Optimal Control; H2/LQG control; Fuzzy Control and also Artificial Neural Network (ANN) control strategies. Some of these control strategies will be applied later in the R&D program in order to understand the pros and cons of each strategy; however, in the current numerical study only a control based upon Lyapunov stability theory will be presented.

In the context of the dynamic behaviour of bridges, equipped with adaptative protection systems, a very special velocity displacement and displacement dependent semi-active control algorithm has been developed and successfully applied (Oliveira and Guerreiro [17], Guerreiro et al. [18], Oliveira et al. [19], Oliveira [20]).

5.2 Some numerical results using Lyapunov Based Control

Lyapunov direct approach was used as a possible semi-active control of MR dampers during the development of control strategies for these devices (Dyke and Spencer [21]). This approach is classified as a bang-bang controller and is dependent on the sign of the measured force and on the states z of the system. According with this approach, it is necessary to define a Lyapunov function or V(z) that is a positive definite function of the states z of the system. If the rate of change of the Lyapunov function is negative semi-definite, the origin is stable in the sense of Lyapunov. Therefore, control inputs for the MR damper must be selected in order to make V as negative as possible. In this case, and following previous research in this filed, the Lyapunov function was chosen of the form:

$$V(z) = \frac{\|z\|_p^2}{2} \tag{14}$$

where $\|z\|_p$ is the P-norm of the z-states defined by

$$\|z\|_p = [z' P z]^{0.5} \tag{15}$$

and P is a real, symmetric, positive definite matrix. To ensure that de derivative of V is negative definite, the matrix P is found using the Lyapunov equation

$$A'P + PA = -Q_p \tag{16}$$

for a positive definite matrix Q_p. The derivative of the Lyapunov function for a solution of Eq. (11) is then

$$\dot{V} = \frac{1}{2} z' Q_p \, z + z' P B \, f + z' P E \, \ddot{x}_g \tag{17}$$

Therefore, the control law that will minimized this function is

$$v = V_{\max} H \left(-z' P B f \right) \tag{18}$$

where H is the Heaviside step function. To implement this algorithm, a Kalman filter was used to estimate the states based on the available measurements (MR damper displacements and structural accelerations).

To study the response of the model structure with the semi-active controller, a few characteristic earthquake records were considered; those will be also input in the Quanser shaking table of FEUP-Covicocepad laboratorial facilities, in order to experimentally calibrate and numerically compare different control strategies. Herein, just the El Centro earthquake record was selected as input (Figure 26).

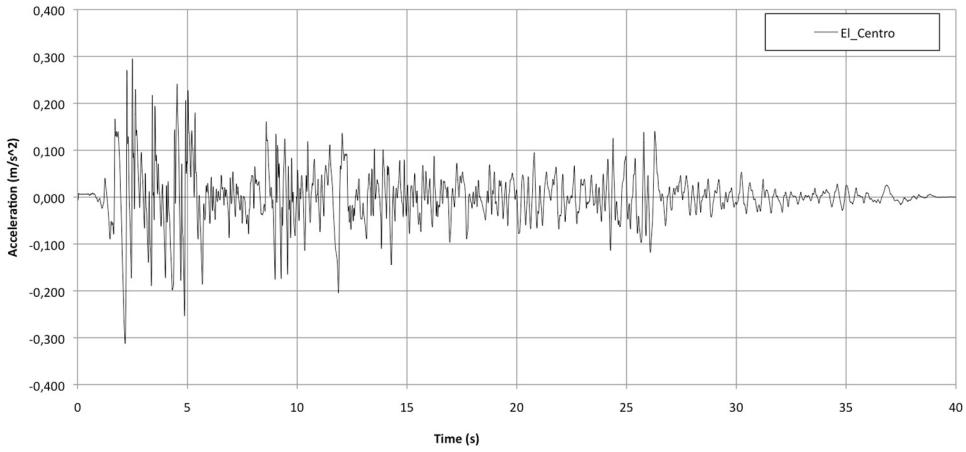

Figure 26: El Centro earthquake signals for semi-active control.

The acceleration at the 3rd floor was selected as the parameter (output) to verify the efficiency of the control law. Some results of this numerical analysis are plotted in Figures 27 and 28, respectively for the 3rd floor horizontal displacement and acceleration, for uncontrolled and controlled scenarios.

As expected, the semi-active control based on Lyapunov stability theory was successfully applied. The 3rd floor lateral displacement and acceleration of the building were reduced significantly during the earthquake duration.

Although the main objective of this analysis is to validate the efficiency of the Lyapunov control strategy it is clear that further numerical and experimental research must be carried out. Since this is an ongoing research program, the next step will be the implementation of new control strategies such as the Clipped-Optimal and also a Fuzzy controller.

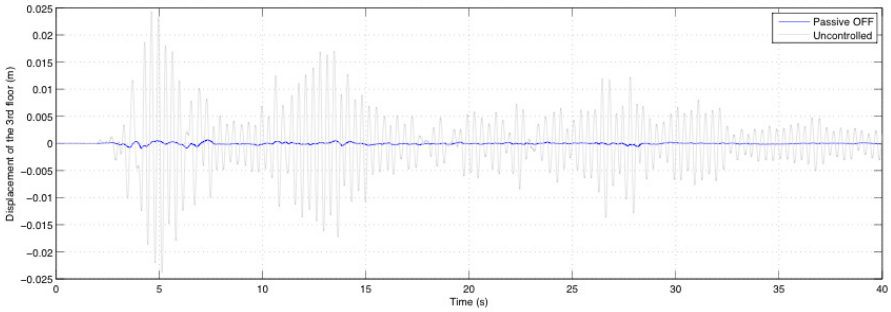

Figure 27: Displacement of the 3rd floor with semi-active control.

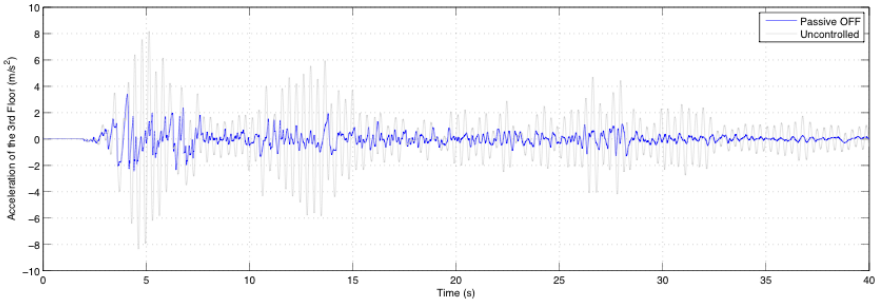

Figure 28: Acceleration of the 3rd floor with semi-active control.

CONCLUSIONS

After an initial contextualization with the R&D activity within COVICOCEPAD project, this paper addresses the vibration control of a 3-DOF experimental metallic frame with a MR damper. The MR damper was tested to find the dynamic properties and a numerical model was developed to simulate its behaviour. System identification allowed obtaining the dynamic response of this structural system. The MR damper was then assembled in the scaled frame and a new identification procedure was carried out to verify the influence of this device in the frame dynamic behaviour. In a numerical example the three-story structure was controlled using a MR damper on the first floor. The simulated results show that the control algorithm, based on Lyapunov stability theory, resulted in an improvement over the uncontrolled system.

ACKNOWLEDGEMENTS

This work reports research developed under the R&D Eurocores Project COVICOCEPAD within the S3T Program, approved independently by European Science Foundation (ESF, Strasbourg), financially supported by portuguese "FCT – Fundação para a Ciência e a Tecnologia" (Lisbon – Portugal) under *Programa Operacional Ciência e Inovação 2010* (POCI 2010) of the *III Quadro Comunitário de Apoio* funded by FEDER, under the EC Sixth Framework Program.

REFERENCES

[1] R.C. Barros, P. Belli, I. Corbi and M. Nicoletti – "Large Scale Risk Prevention", *International Journal of Earthquake Engineering and Engineering Seismology*, European Earthquake Engineering 1.04, ISSN 0394-5103, Vol. XVIII, No.1, pp. 10-19, Patròn Editore, Bologna, Italy 2004.

[2] R.C. Barros, R. Bairrão, F. Branco, I. Corbi, M. Kemppinen, G. Magonette, F. Paulet and G. Serino – "Implementation of Structural Control", *International Journal of Earthquake Engineering and Engineering Seismology*, European Earthquake Engineering 2.05, ISSN 0394-5103, Vol. XIX, No.2, pp. 51-68, Patròn Editore, Bologna, Italy 2005.

[3] R.C. Barros, A. Baratta, O. Corbi, M.B. Cesar, M.M. Paredes – "Some Research on Control of Vibrations in Civil Engineering under COVICOCEPAD Project", *Third International Conference on Integrity Reliability & Failure* (IRF 2009), Editors: J.F. Silva Gomes and Shaker A. Meguid, Porto-Portugal: 20-24 July 2009.

[4] F. Naeim and J.M. Kelly – *Design of Seismic Isolated Structures: from Theory to Practice*, John Wiley & Sons Inc., New York - USA, 1999.

[5] T.T. Soong and G.F. Dargush – *Passive Energy Dissipation Systems in Structural Engineering*, John Wiley & Sons Ltd, Chichester - England, 1999.

[6] R.C. Barros and M.B. César – "Seismic Behaviour of an Asymmetric Three-Dimensional Steel Frame with Base Isolation Devices"; in: *Computational Structures Technology*; Editors: B.H.V. Topping, G. Montero and R. Montenegro; Paper 252, Civil-Comp Press, Stirlingshire, Scotland, 2006.

[7] M.B. César and R.C. Barros – "Influence of Resistant Cores Location on the Seismic Response of a R/C 3D-Frame Equipped with HDRB Base Isolation Devices"; in: *Civil Engineering Computing*; Editor: B.H.V. Topping; Paper 199, Civil-Comp Press, Stirlingshire, Scotland, 2007.

[8] E. Figueiredo and R.C. Barros – "An Insight on the Influence of Damping in Seismic Isolation", in: *Civil Engineering Computing*, Editor: B.H.V. Topping, Civil-Comp Press, Paper 201, Civil-Comp Press, Stirlingshire, Scotland, 2007.

[9] A. Baratta and I. Corbi – "On the optimal design of structural base isolation devices"; in: *Computational Mechanics*: 283-285; Edts: E. Lund, N. Olhoff, J. Stegmann; Aalborg University, Denmark, 2002.

[10] A. Baratta and I. Corbi – "Optimal Design of Base-Isolators in Multi-Storey Buildings", *Int. J. Computers & Structures*, vol. 82, Issues 23-26: 2199-2209, Elsevier, 2004.

[11] R.C. Barros – "Seismic Response of Tanks and Vibration Control of their Pipelines", *Journal of Vibroengineering*, Vol. 4, 2002 - No. 1 (8), Index 136, pp. 9-16, Proceedings Research Center of the Public Institution Vibromechanika, Vilnius, Lithuania, 2002.

[12] R.C. Barros – "Project COVICOCEPAD under Smart Structural Systems Technologies of Program Eurocores"; World Forum on Smart Materials and Smart Structures Technologies (SMSST-2007) Chonqing and Nanjing (China), 22-27 May 2007; in: *Smart Materials and Smart Structures Technology*; Editors: M. Tomizuka, B.F. Spencer, C.B. Yun, W. Chen, R. Chen; Taylor & Francis Ltd, 2008.

[13] S.J. Dyke, B.F. Spencer, M.K. Sain and J.D. Carlson – "Modeling and Control of Magneto-Rheological Dampers for Seismic Response Reduction", *Smart Materials and Structures*, Vol. 5, pp. 565-575, 1996.

[14] D.J. Ewins - *Modal Testing: theory, practice and application*, 2nd edition, Research Studies Press Ltd., England, UK, 2000.

[15] L.M. Jansen and S.J. Dyke – "Semi-active control strategies for MR dampers: a comparative study", *ASCE Journal of Engineering Mechanics*, Vol. 126, No. 8, pp. 795-803, 1999.

[16] C. Kang-Min, C. Sang-Won, J. Hyung-Jo and L. In-Won – "Semi-Active Fuzzy Control for Seismic Response Reduction using Magneto-Rheological Dampers", *Earthquake Engineering and Structural Dynamics*, Vol. 33, pp. 723-736, John Wiley & Sons, Ltd., 2004.

[17] C. Oliveira and L. Guerreiro – "A Velocity and Displacement Dependent Semi-active Control Algorithm", *First European Conference on Earthquake Engineering and Seismology*, Geneva, 2006.

[18] L. Guerreiro, R.C. Barros and R. Bairrão – "Algorithms for Semi-Active Devices Control", *Proceedings of ECCOMAS Thematic Conference "Computational Methods in Structural Dynamics and Earthquake Engineering"* (COMPDYN 2007), Ed.: M. Papadrakakis, D.C. Charmpis, N.D. Lagaros, V. Tsompanakis; Rethymno, Creta (Greece), 13-16 June 2007, Book of Abstracts pp. 262, Full paper 1733 – 6 pages, 2007.

[19] C.F. Oliveira, R. Bairrão, R.C. Barros and L. Guerreiro – "The New Generation of Seismic Semi-Active and Active Protection Systems"; *Proceedings of the 4th European Conference on Structural Control* (4ECSC), Paper 227, St Petersbourg, Russia, 8-12 September 2008.

[20] C. Oliveira – "Dynamic Behaviour Analysis of Bridges with Adaptative Protection Systems", *PhD Thesis submitted at the Technical University of Lisbon*, IST, Lisbon, 2008.

[21] S.J. Dyke and B.F. Spencer Jr. – "A Comparison of Semi-Active Control Strategies for the MR Damper"; *Proceedings of the IASTED International Conference*, Intelligent Information Systems, The Bahamas, Dec. 8–10, 1997.